



Morphology of diblock copolymers via thermal and solvent annealing

Emma Cottenham, University of Durham

September 7, 2016

Abstract

The morphology of block copolymer, polystyrene-block-poly(methyl methacrylate) (PS-*b*-PMMA), is investigated, post deposition on thin silicon films. Two main annealing processes are used, and it is found that solvent annealing with acetone constructs the most stable, structured morphologies. Varying concentrations alters the structure significantly; the optimal hexagonally packed, 'perpendicular cylindrical' structure is constructed using a 9g/l solution, with an annealing time of 4 hours. The optimal 'perpendicular lamellar' structure is determined using a solution with concentration 12 g/l, annealed for 2 hours. Experimentation also displays some evidence that spray deposition onto a PS-*b*-PMMA sample coats only one of the polymers.

Contents

| | | |
|----------|---------------------------------|-----------|
| 1 | Introduction | 3 |
| 2 | Theory | 3 |
| 2.1 | AFM | 3 |
| 2.2 | Thermal Annealing | 4 |
| 2.3 | Solvent Annealing | 4 |
| 3 | Method | 4 |
| 3.1 | Preparation | 4 |
| 3.2 | Analysis | 5 |
| 3.3 | Solvent Annealing | 5 |
| 4 | Results & Discussion | 5 |
| 4.1 | Solvent annealing | 7 |
| 4.2 | Spray Deposition | 10 |
| 5 | Conclusion | 11 |

1 Introduction

Block copolymer (BCP) films are of interest due to their potential to self-orient in a highly regular way. This high level of control over such a nanostructure is desirable when working towards smaller-structured electrical and optical devices. One example of harnessing the BCP morphology is terabit-level memory storage. [1] A difficulty with this, however, is that although the BCP samples may show good short-range ordering - the long-range ordering is not always sufficient. Slight inconsistencies and defects are common within a large scale sample.

In this work, block copolymer films will be studied both before and after two main methods of annealing; thermal and solvent. The morphology after annealing at various temperatures and for different periods of time will be investigated in order to find well-structured, reproducible sample morphology.

2 Theory

Block copolymers consist of two subchains, connected via a covalent bond. Block copolymer films are subject to some degree of confinement, types of which are typically split into two categories. The first considers a film between two fixed interfaces, referred to as 'hard' confinement. The second considers 'soft' confinement, in which a film lies between one fixed interface, and one air interface (referred to as the 'free surface'). In this work, solely films under soft confinement are considered.

Due to this confinement, compression and stretching of the polymer chains within the film is not energetically favourable. [2] Instead, the polymers self-assemble into certain structures which are energetically favourable at the substrate or air interface. Usually, PS and PMMA would separate on a macroscopic scale. However, due to the connected nature of the polymers, they undergo microphase separation. [3] If conditions such as the thickness and interfacial energies are appropriate, this microphase separation yields a nanopatterned substrate.

The shape and size of the patterns, and hence the domain period, are highly dependent upon the polymer choice. In this experimentation, two polystyrene-block-poly(methyl methacrylate) (PS-*b*-PMMA) are used, with block ratio 280/290. The PMMA has a double oxygen bond, making it polar. The substrate used here is made of Silicon and is hence also polar. Thus, it is energetically favourable for PMMA to move to the substrate, due to dipole-dipole interactions between the partial negative charges. Conversely, non-polar PS will move to the air interface.

2.1 AFM

Atomic force microscopy (AFM) is the most commonly used technique to study the morphology of BCP's, as it is non-destructive. AFM, in non-contact mode, produces phase images by oscillating a sharp tip attached to a cantilever above the sample being

investigated. The oscillation frequency is altered by the presence of harder or softer features, hence building up an image of the morphology. [4] However, one downside of this method is that it can be dependent upon imaging parameters. [5] Further, it does not take the whole sample into consideration, but only a small section. Alternatives to AFM imaging include scanning electron microscopy, and grazing incidence X-ray scattering.

In this experimentation, data was recorded from the AFM as phase and height images.

2.2 Thermal Annealing

Post deposition onto the substrate, the polymer solution is generally set in a disordered structure. If taken to above the glass transition temperature of the system, it is possible for the polymers to become mobile and structurally transform. This is because above T_g , it becomes easier for polymer strings to rotate about single bonds. [6]

2.3 Solvent Annealing

During SVA, the exposure to solvent vapours causes the polymers to become mobile upon the substrate. This is because, for this case, the glass transition temperature of the polymers is reduced to room temperature. Thus, as the solvent evaporation process occurs, the polymer chains are able to form ordered structures. [7] Within the literature, it is also indicated that these ordered structures may form more quickly than for other annealing processes. [4] A complete understanding of the SVA process, however, has not been solidly determined. This is because there is currently no standardised method for the process, and in most cases no precisely documented connection between the morphology of the swollen and final dried films.

3 Method

3.1 Preparation

A fundamental attribute in BCP film preparation is the choice of substrate, as each forms a unique interface with the polymer(s) [7]. Silicon wafers were prepared via placement in an ultrasonic bath, containing acetone, for 15 min. After this time, the wafers were thoroughly cleaned with acetone, isopropanol and distilled water sequentially and dried using N_2 gas. This process was of high importance in order for the surface of the substrate to be clear of impurities and dust for optimal coating.

A stock solution was prepared by accurately weighing 125mg of the polymer PS-*b*-PMMA 280/290, and combining it with 2.5ml of toluene. These were then mixed upon a vibrating stage, moving at around 600 RPM for 15 mins, or longer if the solution did not look uniform. This stock solution was then combined with a calculated level of toluene in order to prepare various other concentrations.

A spin-coating technique was adopted to prepare the block copolymer films; 150 μ l of the prepared polymer solution was deposited onto the wafer surface, and the rotation rate set to 3000 RPM. Higher spinning speeds give rise to thinner films, by the relationship $t \propto \sqrt{f}$, where t represents the film thickness, and f the frequency of rotation. Thus, this speed was chosen as the optimal. The film thickness can also be controlled dependent upon the concentration of the polymer solution, through a linear relationship; $t \propto c$, where c represents the concentration. Centripetal acceleration during spin coating causes the solution to spread across the wafer, driving off the acetone via evaporation and leaving behind a polymer layer. [4]

3.2 Analysis

Measurements of thickness, RMS roughness and domain period could be obtained using AFM measurements. Inconsistencies such as background and cantilever movement were corrected for in the AFM data. Thickness measurements were determined by creating a scratch on the surface of the sample. This moved away the polymer top surface, and a simple scan crossing both the scratched and unscratched area enabled a thickness measurement to be calculated.

3.3 Solvent Annealing

A solvent vapour annealing process was used to order some of the samples. These samples were placed in a sealed glass container, upon a raised platform. The container was partially filled with acetone, to a level half way below the platform. This was chosen as an acceptable volume as there was solvent left at the end of the annealing period. Whilst the solvent annealing process occurs in a closed container, the vapour pressure reaches thermodynamic equilibrium with the liquid phase. Hence, as long as there is acetone remaining within the container, the vapour pressure does not depend upon the amount of solvent initially placed in the container (within reason). During this process, acetone was used as the solvent because it is known to make the PMMA within the BCP mobile.

The samples were taken to be initially 'good' when they were of homogenous colouring. The colours observed on the wafers are caused due to thin-film interference; thus a consistent colour across the sample indicates a constant film thickness.

4 Results & Discussion

During initial experiments an incremental range of concentrations were studied, in order to create a concentration line of thermally annealed samples. Namely, 10-50g/l in steps of 10g/l. This process was performed for various temperatures and times.

It was found that the thermal annealing process, for both short (4h) and longer (24h) times did not substantially improve the structure of the samples. This can be observed

from Fig 1, in which the structure does not appear to change between the two concentration series. This is reinforced by Fig 2, in which the fast Fourier transform (FFT) of both samples displays a very similar shape - indicating a similar periodicity.

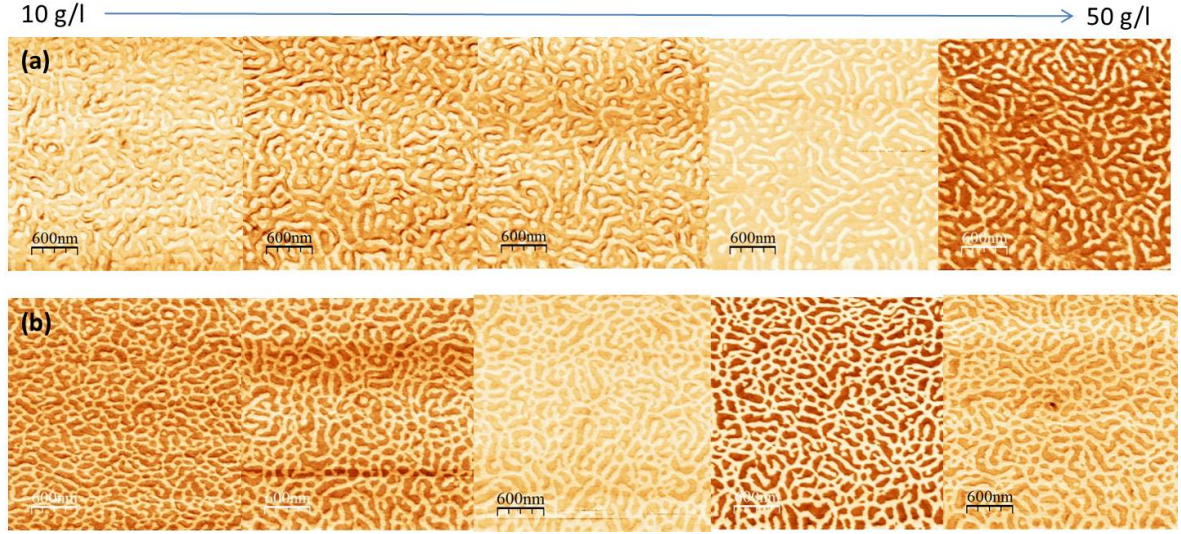


Figure 1: Displaying the concentration series of samples prepared with PS-*b*-PMMA 280/290. This ranges from 10g/l to 50g/l, in steps of 10g/l. (a) Shows before annealing, and (b) after 4h thermal annealing.

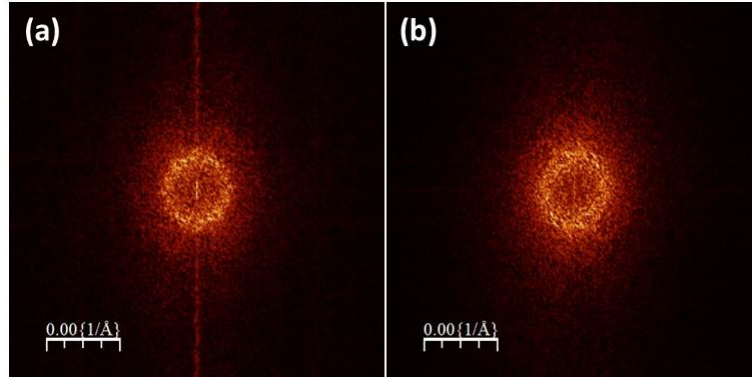


Figure 2: (a) FFT of 40g/l sample before annealing, and (b) after 4h thermal annealing.

It should also be noted that the samples left for a period of 24h began to show worse structure post annealing.

It was noted from literature that optimal results were found when the domain period of the sample matches the thickness. [8] From analysis of the AFM images, the domain period was found to be 139 ± 2 nm. From thickness measurements, this appeared to

coincide with a concentration between 7-14g/l. Therefore, the spin coating technique was used to prepare a concentration series of eight samples, varying from 7g/l to 14g/l. These new samples were further split into multiple 10 x 10mm pieces, in order to anneal them in various ways and compare the final morphologies.

It was found that the new samples produced worse-structured morphology post thermal annealing. This was a similar result to what was found previously for the 24h thermally annealed samples.

4.1 Solvent annealing

A solvent annealing process was attempted using the new concentration of samples. The samples were tested after a period of 2h and 4h. After 2h, a representative selection of the sample group looked to have good ordering. It can be observed from Fig 3 that the BCP film morphology varies significantly along the concentration series. At lower concentrations, a perpendicular cylinder structure can be observed. As one moves through the series, to higher concentrations, both cylindrical and perpendicular lamellar structures are observed - until one reaches 12g/l, where the morphology becomes simply perpendicular lamellae.

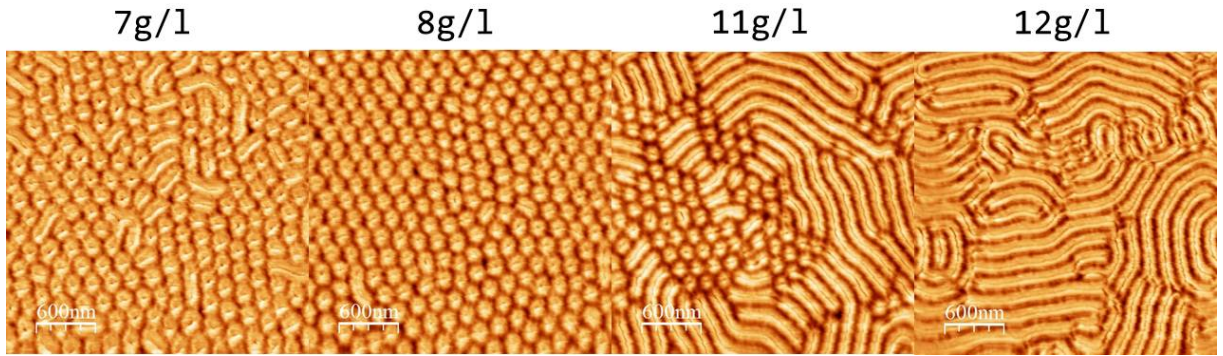


Figure 3: Concentration series showing a representative sample of concentrations, after a 2h solvent annealing process.

A solvent annealing period of 4h has been found as the optimal time to anneal PS-*b*-PMMA samples by another member of the group. Thus, the samples were returned to the container, and left for a further two hours to see whether the structure improved, or how it changed.

After leaving the samples for a further two hours, all samples were studied. This produced a concentration series as can be observed in Fig 4. Comparing the two concentration series, and various other parameters - such as their FFT's - it appears that the 9g/l sample annealed for 4h presents the most consistent cylindrical structure. Further, the 12g/l sample annealed for 2h presents the most ordered perpendicular lamellar morphology. It also appears that the longer the annealing time, the more of one block is

identified at the surface. This can be observed by comparison of the 12g/l sample in both Fig's 3 and 4.

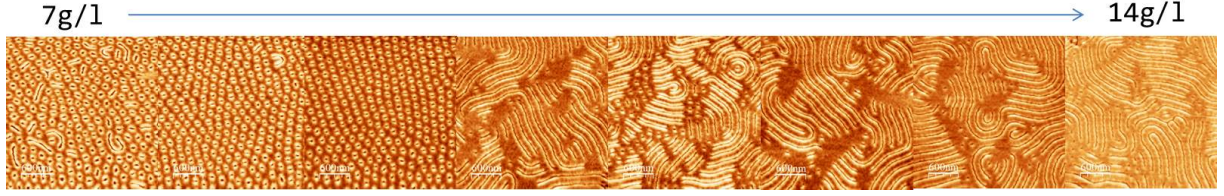


Figure 4: Concentration series after a 4h solvent annealing process.

The reproducibility of these samples was tested. This involved re-creating the PS-*b*-PMMA with toluene stock solution, and re-making the different concentrations. Unfortunately, the first attempt at reproducing these results was unsuccessful. The 9g/l sample shows a similar structure to before, but seems to be a combination of the two morphologies. This inconsistency is believed to be due to the stock solution not mixing completely. This time, the stock solution was mixed for the same period as previously, but was observed to have small pieces of PS-*b*-PMMA remaining undissolved. Thus, the solution was left to mix overnight. It was observed to still have the same inconsistencies in its homogeneity. If the diblock is not completely dissolved, then a different concentration will have been produced, hence creating a different morphology.

A second set of samples were created using a more homogenous stock solution. These samples produced good morphology, and follow patterns as expected. It can be seen in Fig 5 that the 9g/l sample produces an almost consistent cylindrical morphology, and the 12g/l a perpendicular lamellar morphology.

The structure presented post solvent annealing is more uniform, and hence more useful for future application in technology.

By comparison of the AFM phase images in this section and the previous, it can be noted by eye that the morphology of the solvent annealed samples show better order. This can also be observed from the FFT samples, with similar concentration, after the two processes, as displayed in Fig 6. The FFT after oven annealing is more diffuse, showing a slight elongation along the vertical axis - but no distinct directionality. After solvent annealing the FFT follows a more precise ring structure. The six bright spots around the ring indicate the six periodicities along directions originating from the hexagonal polymer structure.

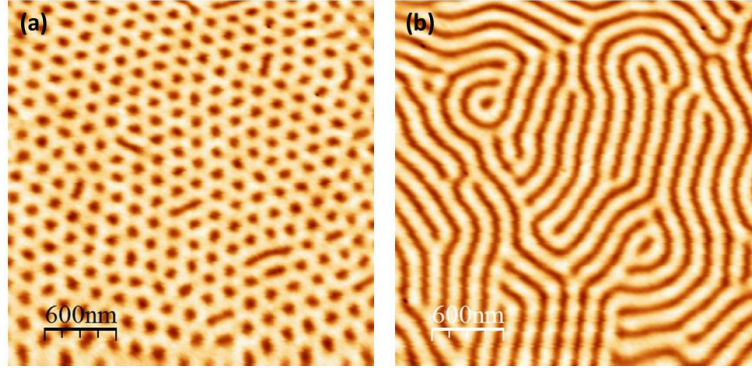


Figure 5: Samples reproduced with a solvent annealing method (a) presents 9g/l annealed for 4h, (b) 12g/l annealed for 2h.

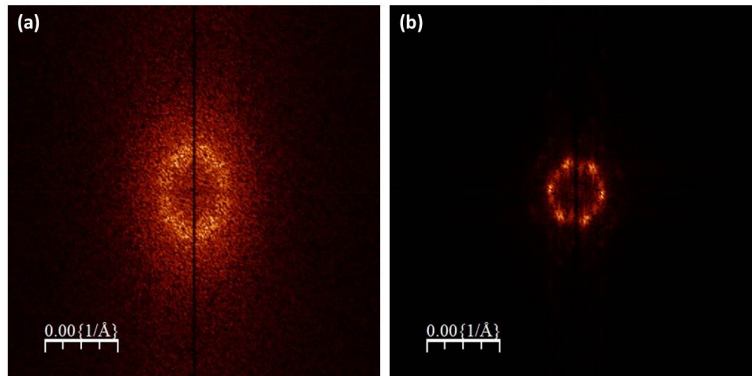


Figure 6: (a) FFT of 10g/l sample post oven annealing, and (b) FFT of 9g/l sample post solvent annealing.

4.2 Spray Deposition

It was deemed interesting to attempt to spray silver salt solution on a particularly ordered sample. This was to determine whether the spray was deposited on only one of the polymers, and if so - which of the polymers. It can be observed from Fig's 7 and 8 that the spray appears to deposit upon the highest polymer layer. However, this was not consistent throughout the sample. Some areas of the sample were damaged, and in others the structure completely destroyed. This was believed to be due to the ethanol content in the spray that was deposited. This theory was tested by spraying solely ethanol onto a well-ordered sample. Through AFM analysis post-ethanol spraying, the nanostructure was seen to be destroyed in a similar way. This indicates the ethanol content was a cause towards the discrepancies in the structure post-spraying.

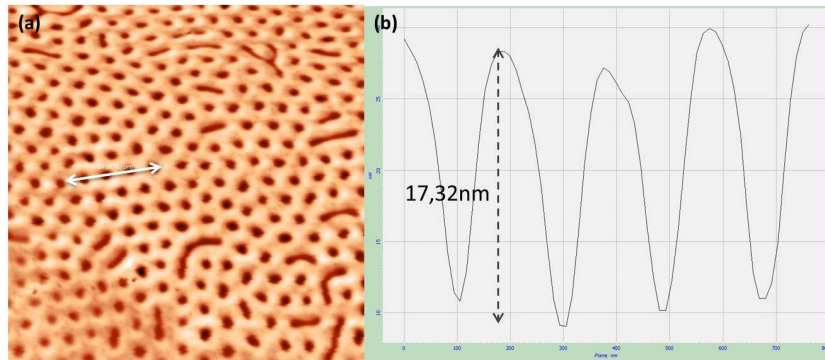


Figure 7: 7g/l sample post spray deposition. Image (a) obtained using AFM measurements displays the deposition pattern of the spray, and an arrow is included to indicate where the line profile (b) was taken.

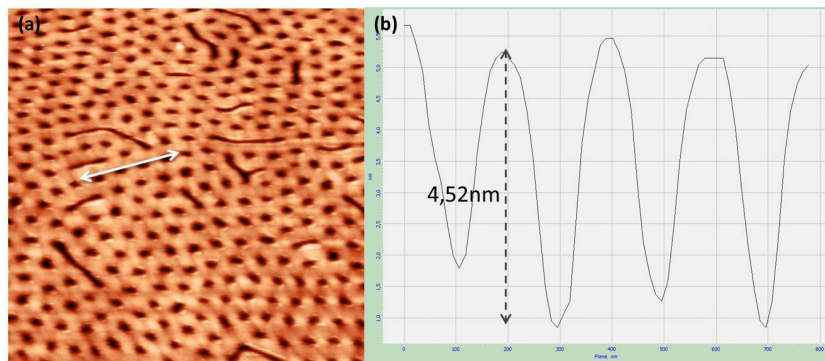


Figure 8: 7g/l sample pre spray deposition, used for comparison to the previous figure. Image (a) obtained using AFM measurements displays the morphology of the sample, and again an arrow is included to indicate where the line profile (b) was taken.

5 Conclusion

In this work, a quick, effective and reproducible way of obtaining both stable cylindrical and perpendicular lamellar nanostructures was documented. Many variations on two annealing techniques were explored; varying both the time and temperature during thermal and solvent annealing processes. Solvent annealing was found to be of more use than thermal annealing in producing regular structures. It produced annealed samples with superior order; in both the short and long range. It was also less time-consuming and more consistent.

A brief look at spray deposition onto a well-ordered sample presents scope for further work. Initial tests showed promise, and deposition onto only one of the polymers was observed in most places. However, more research must be conducted to perfect this technique - potentially using a chemical other than ethanol in the preparation of the silver spray solution.

References

- [1] M. J. Fasolka and A. M. Mayes, “Block Copolymer Thin Films: Physics and Applications,” *Annu. Rev. Mater. Res.*, vol. 31, pp. 323–55, 2001.
- [2] J. N. L. Albert and T. H. Epps, “Self-assembly of block copolymer thin films,” *Materials Today*, vol. 13, pp. 24–33, 2010.
- [3] T. L. Morkved and H. M. Jaeger, “Thickness-Induced morphology changes in lamellar diblock copolymer ultrathin films,” *Europhysics Letters*, vol. 40, pp. 643–648, 1997.
- [4] I. W. Hamley, “Ordering in thin films of block copolymers: Fundamentals to potential applications,” *Progress in Polymer Science*, vol. 34, pp. 1161–1210, 2009.
- [5] G. Bar, Y. Thomann, R. Brandsch, H. Cantow, and M.-H. Whangbo, “Factors Affecting the Height and Phase Images in Tapping Mode Atomic Force Microscopy. Study of Phase-Separated Polymer Blends of Poly(ethene-co-styrene) and Poly(2,6-dimethyl-1,4-phenylene oxide),” *Langmuir*, vol. 13, pp. 3807–3812, 1997.
- [6] D. Erb, “Highly-Ordered Magnetic Nanostructures on Self-Assembled α -Al₂O₃ and Diblock Copolymer Templates,” *Unpublished doctoral dissertation*, 2014.
- [7] C. Sinturel, M. Vayer, M. Morris, and M. A. Hillmyer, “Solvent Vapor Annealing of Block Polymer Thin Films,” *Macromolecules*, vol. 46, pp. 5399–5415, 2013.
- [8] Y. Xuan and et. al, “Morphology Development of Ultrathin Symmetric Diblock Copolymer Film via Solvent Vapor Treatment,” *Macromolecules*, vol. 37, pp. 7301–7307, 2004.